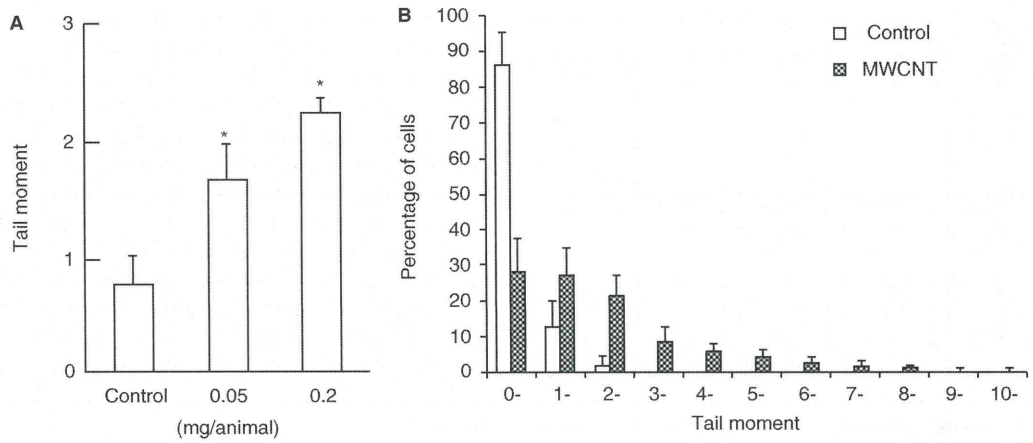

Figure 2. DNA damage in the lungs of ICR mice intratracheally instilled with MWCNTs. DNA damage was measured by comet assay. (A) The mean values of DNA tail moment in the lungs with or without a 3 h MWCNT treatment at 0.05 or 0.2 mg/animal. The values represent the mean of five animals ± SD; $*p < 0.01$, by Dunnett's test after one-way analysis of variance *versus* the corresponding vehicle control mice. (B) The percentages of cells containing a given comet tail moment at a dose of 0.2 mg/animal.

Histopathological evaluation

For histopathological evaluation, lungs obtained from *gpt* delta mice with or without nanoparticle instillation ($n = 2$ or 3) were fixed in 10% neutral buffered formalin, embedded in paraffin blocks, and routinely processed to haematoxylin and eosin-stained sections.

Immunohistochemical analysis of inflammation factors

To investigate nitric oxide production after nanoparticle exposure, immunohistochemical staining of inflammation factors, such as inducible NO synthase (iNOS) and nitrotyrosine (NT), in the lungs of *gpt* delta mice treated with MWCNTs were examined, using a procedures reported previously (Totsuka et al. 2010; Porter et al. 2002).

Statistical analysis

The data obtained from the comet assay were expressed as the mean ± standard deviation (SD). Dunnett's test after one-way analysis of variance was used to test for significant differences in tail moment and percentage of DNA in tail. The data from the micronucleus test were expressed as the mean ± SD of three independent experiments. The data from the SCE test were expressed as the mean ± SD of at least 50 cells. The data from the *gpt* and Spi$^-$ mutation assays were expressed as the mean ± SD. The data were statistically compared with the corresponding solvent control using the F test before application of the Student's *t*-test. Mutational spectra were compared using Fisher's exact test (Carr & Gorelick 1996). *P* values < 0.05 were considered to indicate statistical significance.

Results

Micronucleus test

To investigate the genotoxicity/clastogenicity of MWCNTs, micronucleus-inducing activity was analysed using a human lung cancer cell line, A549. A 6 h treatment with MWCNTs, at a concentration of 20 μg/mL or higher, inhibited A549 cell growth to around 70% of control levels. As shown in Figure 1, MWCNTs increased the number of micronucleated cells in a dose-dependent manner. The frequency of micronucleated cells in the solvent control was 1.12% and the frequency rose to 8.6% in the 200 μg/mL MWCNT group. Even treatment of 20 μg/mL MWCNT induced micronuclei exceedingly, and these increases were statistically significant ($p < 0.05$).

SCE test

Table I shows the SCE frequency in CHO cells following a 1 h treatment with MWCNTs. An SCE frequency approximately three times the control level was observed in cultures treated with 1.0 μg/mL MWCNTs. This increase was statistically significant ($p < 0.01$) at 0.1 μg/mL or higher concentrations.

In vivo genotoxicity analysed by alkaline comet assay

DNA damage induced by MWCNTs in the lungs was evaluated using a comet assay under alkaline conditions. Figure 2A shows the mean values of DNA tail moment in the lungs with or without a 3 h MWCNT treatment at 0.05 or 0.2 mg/animal. DNA damage observed in the MWCNT-treated group was dose-dependent, and the values of DNA tail moment were significantly increased compared with those of the vehicle control. Also, similar dose-dependent manner was observed in the values of percentage of DNA in the tail (Supplementary Figure 1). Figure 2B shows the percentages of cells containing a given comet tail moment at a dose of 0.2 mg/animal. The numbers of damaged cells were increased by treatment with nanoparticles and damaged cells with high DNA tail moment being extremely rare in the vehicle group.

Quantification of oxidative and lipid peroxide-related DNA adducts

Levels of the DNA adduct analysed in lung DNA extracted from MWCNT-treated mice at 3, 24, 72 and 168 h after exposure are shown in Figure 3. DNA adducts related to oxidative stress and lipid peroxidation (8-oxodG, HεdA, HεdC, HεdG) were all, except HεdG, increased up to 72 h and then slightly less so at 168 h. 8-OxodG was more

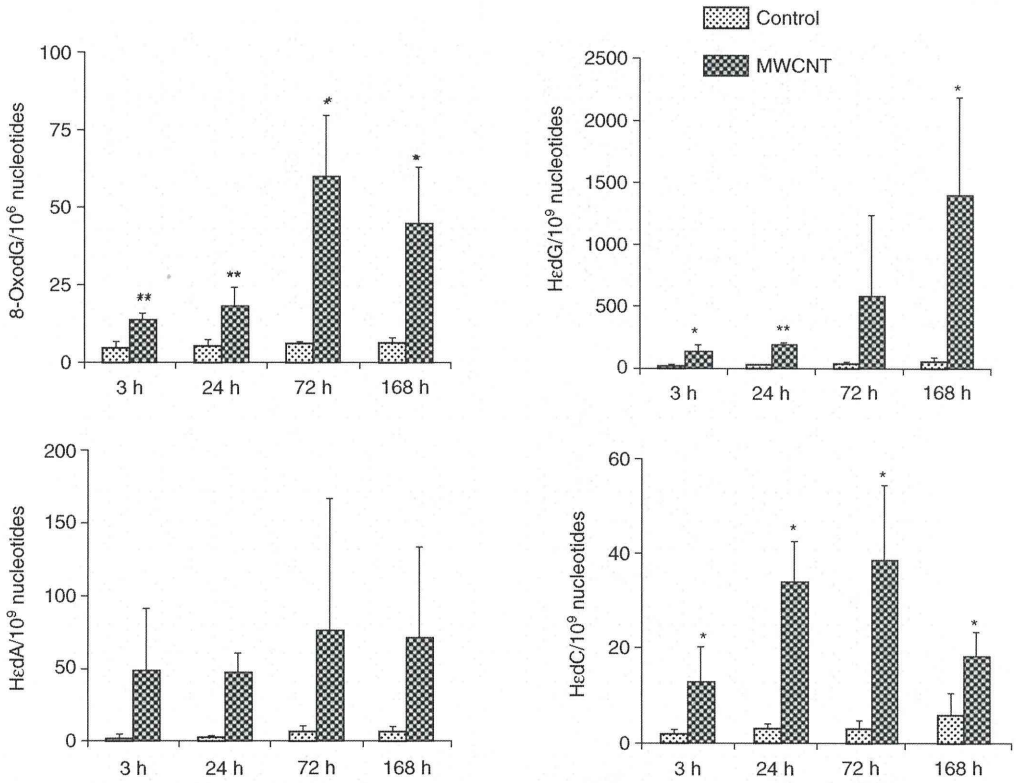

Figure 3. Oxidative and lipid peroxide-related DNA adduct formation induced by MWCNT exposure in the lungs of ICR mice. DNA was extracted from the lungs 3, 24, 72 and 168 h after intratracheal instillation of 0.2 mg of MWCNTs, and was enzymatically digested. Control samples were obtained from the lungs of mice given vehicle for the same durations of MWCNT exposure. 8-OxodG and three types of Hε-adduct were quantified by stable isotope dilution LC-MS/MS. Asterisks (*, **) indicate a significant difference ($p < 0.05$, < 0.01) from vehicle control (treatment with 0.05% (v/v) Tween-80) at same point in the Student's *t*-test.

abundantly found than the Hε–adduct derived from lipid peroxidation.

General observations and histopathological evaluation of *gpt* delta transgenic mice administered with MWCNTs

The body weights of *gpt* delta mice in the vehicle control group were 34.9 ± 1.9 g at the end of the experiment. The body weights of the *gpt* delta mice that received single or multiple doses of 0.2 mg MWCNTs were 75–80% of those in the vehicle control group during or just after the instillations, then gradually returned to normal by the end of the experiment.

There were no obvious histopathological changes in the lungs of Group 1 control mice (Figure 4A). In mice given a single MWCNT administration (0.2 mg/animal; Group 2), infiltration of macrophages phagocytising tubes in the alveolar lumina and walls, and granulation with fibrosis were observed, in association with inflammatory lymphocyte infiltration in macrophage-clustered lesions and around the vessels and bronchi (Figure 4B). Degeneration, enhanced secretion and hyperplasia were found in the bronchial epithelia, and type II alveolar epithelial cells appeared hyperplastic (Figure 4B). The thickening lesions were also seen in the visceral pleurae, which were due to sub-pleural fibrosis with the occasional detection of MWCNTs (Figure 4D and 4E). When MWCNTs were multiply administered (0.2 mg weekly for 4 weeks; Group 4), generally similar findings were observed but with a much higher severity (Figure 4C). Moreover, MWCNTs were deposited in the paratracheal lymph nodes (Figure 4F). Similar findings, but with a slighter degree of particle accumulation and granuloma formation, were observed in the lungs of mice that received two consecutive MWCNT instillations (Group 3; data not shown).

gpt and Spi$^-$ mutations in the lungs of *gpt* transgenic mice treated with MWCNTs

The *gpt* delta transgenic mice were exposed to single or multiple intratracheal instillations of 0.2 mg MWCNTs and the mutations in the lungs were analysed. Data are summarised in Supplementary Table I, and Figure 5 shows the *gpt* mutant frequencies (MFs) in the lungs. The background MF of the lungs was $7.53 \pm 0.91 \times 10^{-6}$. There was no increase in the MF in lungs exposed to single or double doses of MWCNTs. However, four instillations of MWCNTs resulted in a significant increase in the MF, of approximately two-fold compared with that in controls (Figure 5). The Spi$^-$ MFs were measured in the lungs of *gpt* delta mice instilled with MWCNTs, but no increases were observed (data not shown).

To analyse the characteristics of the mutations induced by MWCNTs, the authors tested for 6-thioguanine (6-TG)-resistant mutants using PCR and DNA sequencing analysis. A total of 42 independent 6-TG-resistant mutants derived

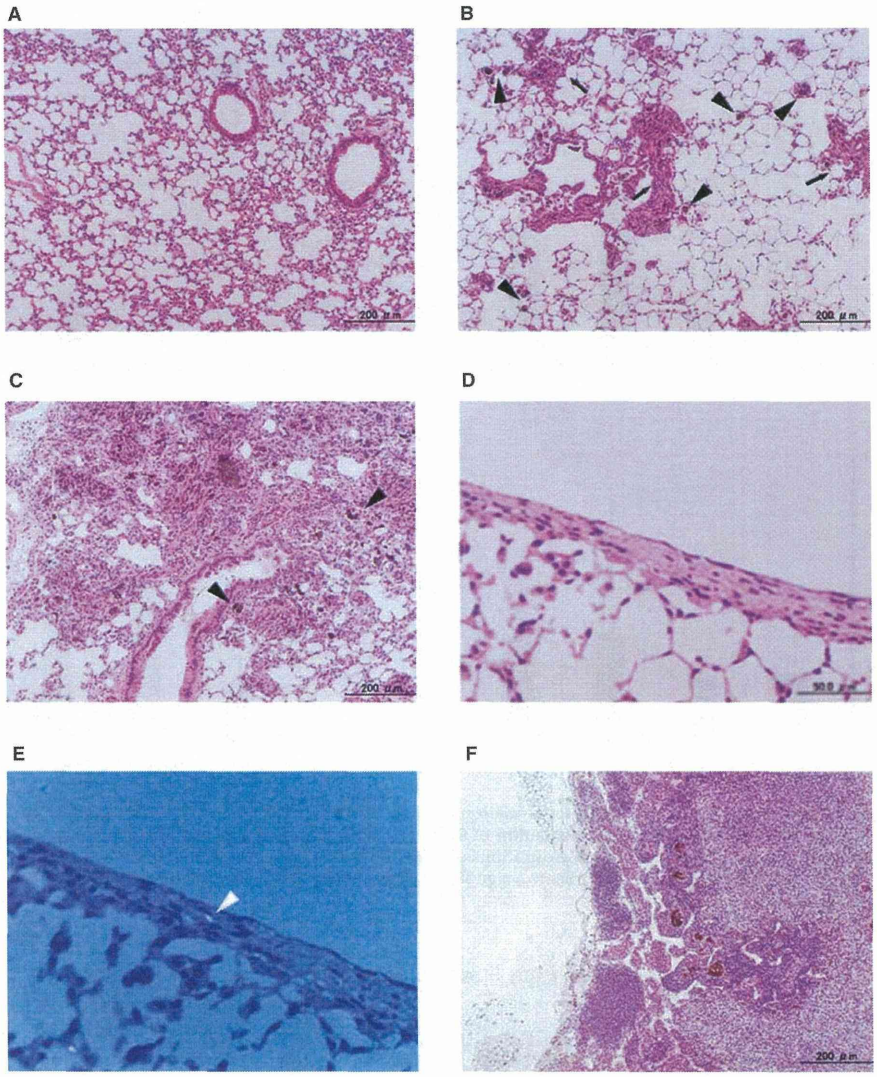

Figure 4. Representative histopathology of the lungs of (A) a control mouse given vehicle (once a week for 4 weeks; killed at the end of month 3); (B) a mouse given a single dose of 0.2 mg MWCNTs (killed at the end of month 3); (C) a mouse given multiple doses of 0.2 mg MWCNTs (once a week for 4 weeks; killed at the end of month 3); (D) a mouse given MWCNT (0.2 mg/head, singly, killed at the end of month 3); (E), a polarisation photomicrograph serial to (D); and (F) a representative paratracheal lymph node of a mouse given multiple doses of 0.2 mg MWCNTs (once a week for 4 weeks; killed at the end of month 3). MWCNT-phagocytised macrophages (black arrowheads) can be observed, and granulation with fibrosis (black arrows) is also found in lungs of MWCNT-instilled mice. In polarisation photomicrograph, MWCNTs is indicated by white arrowhead.

from MWCNT instillations were identified and 24 mutants were identified from vehicle controls. The classes of mutation found in the *gpt* gene are summarised in Table II. Base substitutions predominated in nanoparticle-induced and spontaneous cases. No G:C to C:G transversions were detected in the vehicle control group; however, this type of mutation could be detected in several MWCNT-instilled animals, and p value can be considered significant ($p < 0.05$). The numbers of A:T to T:A transversions and deletions were also slightly increased by MWCNT treatment, though p values were not significant.

Immunohistochemical analysis of inflammation factors

As shown in Figure 6, the pattern of iNOS and NT staining corresponded to the areas of inflammation within the lung parenchyma. In the case of MWCNT exposure, many regions of the lungs stained positively, and intense iNOS and NT staining was mainly localised in test substance-phagocytised macrophages and granulomas (indicated by green arrows). Some alveolar epithelial cells located near granulomas were also stained positive for the iNOS and NT antibodies (indicated by arrowheads). In contrast, no regions stained positively for iNOS were observed in the lungs of vehicle control mice (Figure 6D). Similar results were obtained for vehicle control mice immunoreaction with NT (data not shown).

Discussion

The present study showed MWCNTs to clearly exert genotoxicity in *in vitro* assay systems, significantly inducing

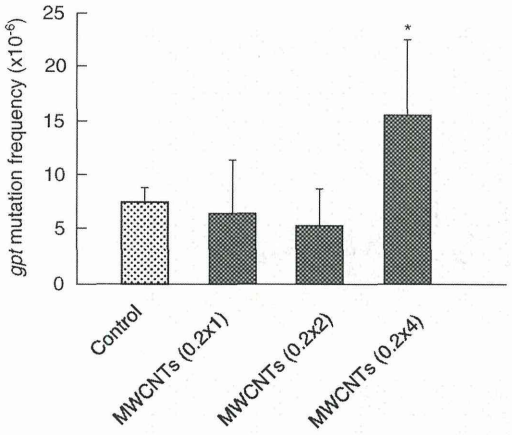

Figure 5. The *gpt* MFs in the lungs of mice after single and multiple intratracheally instillations of MWCNTs. Male mice were treated with a single (0.2 mg) or multiple (0.2 mg × 2 or 4) doses of particles, and mice were sacrificed 12 (single-dose) or 8 (multiple-dose) weeks after particle administration. The data represent the mean ± SD; $*p < 0.05$ by Student's *t*-test *versus* the corresponding vehicle control mice.

micronuclei and enhancing the frequency of SCEs in A549 and CHO AA8 cells. Consistent with this, several studies have reported that MWCNTs can be taken up into many types of cells and demonstrate genotoxicity, including human epithelial lung cells (Wörle-Knirsch et al. 2006), mesothelioma cells (Wick et al. 2007), keratinocytes (Monteiro-Riviere et al. 2005), and normal dermal fibroblast cells (Patlolla et al. 2010b). Recently, several reports have demonstrated that carbon nanotubes induce both clastogenic events and aneugenic events (Muller et al. 2008; Sargent et al. 2009, 2011 unpublished data). Indeed, one of the mechanisms of genotoxicity is considered to be the disruption of mitotic spindles by association with mitotic tubules (Sargent et al. 2009, 2011 unpublished data; Asakura et al. 2010). Moreover, a direct interaction between carbon nanotubes and DNA has also been reported (Li et al. 2005). Other than that, it has been reported that modified gold nanoparticles induce the unfolding of fibrinogen *via* binding and then promote interaction with the integrin receptor Mac1 and induce the release of inflammatory cytokines (Deng et al. 2011). In the present study, no data are available to explain the exact mechanisms of *in vitro* genotoxicity by MWCNTs; however, direct interaction between biomolecules, such as protein and DNA, and MWCNTs might be partly involved for induction of the *in vitro* genotoxicity.

In addition to the *in vitro* genotoxicity, MWCNTs were showed to be genotoxic in the lungs of mice using a comet assay. Under similar conditions, levels of 8-oxodG were significantly increased in MWCNT-treated mice, and the level was maintained for 1 week. The levels of HεdA, HεdC and HεdG also tended to increase. These DNA adducts are derived from lipid peroxidation, suggesting that MWCNTs may induce oxygenation of lipids in tissues caused by generation of reactive oxygen species (ROS). Consistently, it has been reported that the levels of lipid hydroperoxides, which are prominent non-radical intermediates of lipid peroxidation products, were increased in the liver of Swiss-Webster mice intraperitoneally administered with MWCNTs (Patlolla et al. 2010c). Moreover, in the present study, MWCNTs showed mutagenicity in the lungs of *gpt* delta transgenic mice. However, a dose-dependent MF increase was not observed in the lungs of MWCNT-treated groups. The reason is still unclear, but weak responses observed in single or double doses suggested that the degree of DNA damage seems insufficient to fix as mutations, therefore it could not raise MFs more than basal levels under these conditions. Supporting this hypothesis, previous reports have revealed that obvious responses were not observed in either cellular inflammatory end points in bronchoalveolar lavage or pathological changes, such as immune response and fibrosis, in the lungs of animals exposed to low doses of MWCNTs (Ryman-Rasmussen et al. 2009; Pauluhn 2010a). On the other hand, it has also been reported that MWCNTs are difficult to eliminate; it remain in the lungs for a long time and trigger sustained pulmonary inflammation (Ellinger-Ziegelbauer & Pauluhn 2009; Pauluhn 2010a,b). Therefore, to evaluate the effects of MWCNTs with low exposure, it would be preferable to use long-term mutation assay systems. In general, 8-oxodG causes transversion

Table II. Classification of *gpt* mutations isolated from the lungs of control and MWCNT-treated mice.

	Control		MWCNTs		
Type of mutation	No. of mutants (%)	Specific MF† (× 10^{-6})	No. of mutants (%)	Specific MF† (× 10^{-6})	*p* value*
Base substitution					
Transition					
G:C to A:T	7 (29.2)	2.20	11 (26.2)	4.03	0.238
A:T to G:C	2 (8.3)	0.62	2 (4.8)	0.74	1.000
Transversion					
G:C to T:A	8 (33.3)	2.51	10 (23.8)	3.66	0.481
G:C to C:G	0 (0)	0.00	5 (11.9)	1.83	0.02
A:T to T:A	0 (0)	0.00	1 (2.4)	0.37	0.458
A:T to C:G	2 (8.3)	0.62	2 (4.8)	0.74	1.000
Insertion	1 (4.2)	0.32	2 (4.8)	0.74	0.596
Deletion	4 (16.7)	1.26	9 (21.4)	3.29	0.101
Others	0 (0)	0.00	0 (0)	0.00	-
Total	24 (100)	7.53	42 (100)	15.40	0.004

*p values were determined using Fisher's exact test according to Carr and Gorelick; †Specific MF was calculated by multiplying the total mutation frequency by the ratio of each type of mutation to the total mutation.

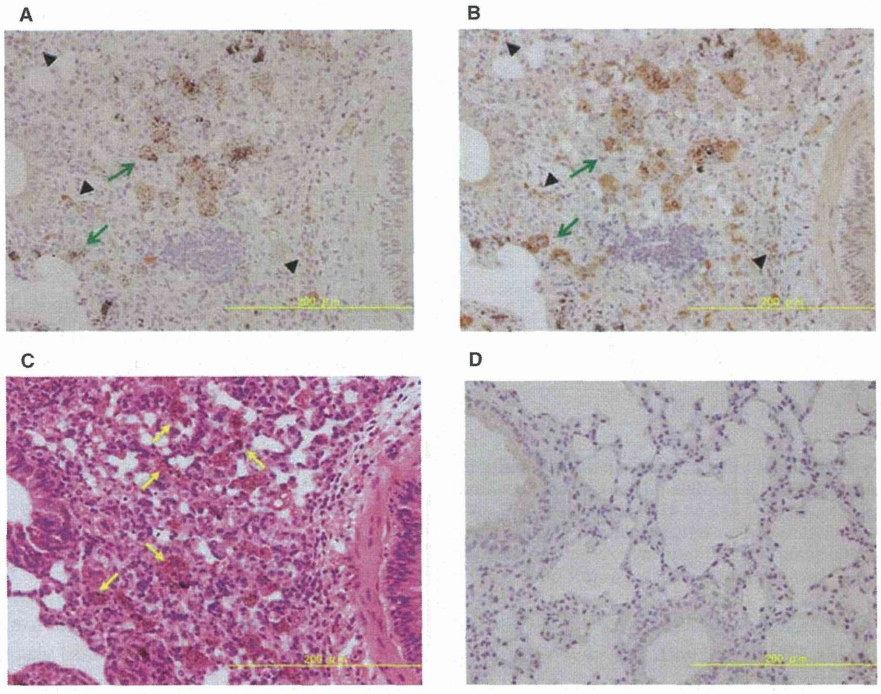

Figure 6. Immunohistochemical localisation of iNOS and NT. The panels show the alveolar region in a mouse exposed to MWCNTs, with positive staining for iNOS (A) and NT (B), and a haematoxylin and eosin stain (C). The black-coloured material is MWCNTs. Note the intense staining for iNOS and NT in both the granulomatous regions (green arrows) and epithelial cells (black arrowheads). The granulomatous regions in (C) are indicated by yellow arrows. Panel (D) shows the alveolar region in a vehicle control mouse with no significant staining for iNOS. Scale bars = 200 μm.

mutations (G:C to T:A) in DNA because it can base pair with adenine as well as cytosine (Shibutani et al. 1991; Moriya 1993). Recently, it has been reported that HεdC predominantly induces C to A or T mutations in human cells (Pollack et al. 2006; Yang et al. 2009). However, the most prominent mutation type induced by MWCNTs was G:C to C:G transversions, as was the case in our previous reports on fullerene and kaolin (Totsuka et al. 2009). In addition, Jacobsen et al. have recently reported that carbon black (Printex 90) induced base substitutions in the *cII* gene in FE1-Muta™Mouse lung epithelial cells (Jacobsen et al. 2011). The significant increases in these mutations were G:C to T:A, G:C to C:G and A:T to T:A, being similar to the results. Moreover, these mutations might be considered a hallmark of oxidative stress conditions. Oxidative products of guanine other than 8-oxodG, such as imidazolone, oxazolone (Oz), spiroiminodihydantoin, (Sp) and guanidinohydantoin (Gh), are now thought to be important causes of G to C transversions in translesion synthesis systems (Kornyushyna et al. 2002; Cadet et al. 1994; Goyal et al. 1997; Ye et al. 2003; Burrows et al. 2002; Kino & Sugiyama 2005, 2001; Kino et al. 2004). Therefore, it is suggested that Oz, Sp and Gh formation by MWCNTs might contribute to induce G:C to C:G transversions. Thus, it is important to analyse the formation of Oz, Sp and Gh in the lungs of mice treated with MWCNTs. The following hypotheses can be suggested to account for the *in vivo* genotoxic effects of MWCNTs through oxidative stress: (i) nanoparticles might trigger ROS production by iron-catalysed Fenton reactions; or (ii) nanoparticles could accumulate in cells because of phagocytosis and then enhance the production of ROS by NADPH oxidase (Aust 1994; Mossman & Gee 1993).

In the present study, inflammatory changes were introduced in the lungs of MWCNT-treated mice. Histologically, the infiltration of macrophages phagocytising tubes is thought to be a trigger, and it is clear that this inflammation originates from the host reaction towards foreign bodies. Bronchial and alveolar epithelia were influenced secondarily. It is noteworthy that the induction of lung inflammation was dependent on the total administered dose of MWCNTs. These histological findings are in line with those in previous reports indicating the induction of inflammation in the lungs by MWCNTs (Aiso et al. 2010; Ma-Hock et al. 2009; Pacurari et al. 2010; Poland et al. 2008; Takagi et al. 2008; Sakamoto et al. 2010). Intratracheally administered MWCNTs were shown to reach the visceral pleura, causing its thickening (Ryman-Rasmussen et al. 2009). Moreover, nitric oxide is known to be produced by activated macrophages in inflamed organs (Porter et al. 2006). In fact, iNOS- and NT-positive regions were frequently observed in the lungs of mice exposed to MWCNTs not only in test substance-phagocytised macrophages and granulomas but also in alveolar cells located near substance-phagocytised macrophages and granulomas (Figure 6, indicated by arrowheads). This suggests that MWCNTs induce nitric oxide production and gene mutation in the surrounding alveolar epithelial cells. Moreover, MWCNTs were found in the regional lymph nodes; such tubes would enter the lymphatic circulation and may then be distributed systemically.

Recently, many types of modified MWCNTs have been produced because of increases in their functionality and

more widespread use (Chen et al. 2010). However, the genotoxicity of these modified nanomaterials has yet to be examined. Recent data have shown that the acute toxicity and genotoxicity of MWCNTs could be eliminated by the induction of structural defects after high-temperature treatment (Fenoglio et al. 2008). It has also been reported that MWCNT-induced toxicity, such as oxidative stress and inflammation, was increased by acid-based polymer coating but that coating MWCNTs with a polystyrene-based polymer protected against toxicity (Tabet et al. 2011). To improve their safety for occupational and general users, it is necessary to clarify the genotoxicity of modified MWCNTs.

Conclusions

It has been clearly demonstrated that MWCNTs induce both *in vitro* and *in vivo* genotoxicity. Although the mechanisms are not yet fully understood, oxidative stress and inflammation are likely to be involved. Thus, further studies of the mechanisms of genotoxicity are needed. Moreover, the levels of human exposure to MWCNTs should be studied to enable evaluation of the risk of MWCNTs to human health.

Acknowledgments

We thank Mr Naoaki Uchiya and Ms Hiroko Suzuki for excellent technical assistance.

Declaration of interest

The authors report no conflicts of interest. The authors alone are responsible for the content and writing of the paper. This study was supported by Grants-in-Aid for Cancer Research, for the U.S. - Japan Cooperative Medical Science Program, for Research on Risk of Chemical Substances from the Ministry of Health, Labour, and Welfare of Japan, for Young Scientists (B) 23710084, KAKENHI (23221006) and for the Global COE Program from the Ministry of Education, Culture, Sports, Science and Technology of Japan. The study was also supported by a grant from the Japan Chemical Industry Association (JCIA) Long-range Research Initiative (LRI). Kousuke Ishino is presently the recipient of a Research Resident Fellowship from the Foundation for Promotion of Cancer Research. The findings and conclusions in this manuscript have not been formally disseminated by the University of Shizuoka and should not be construed to represent any agency determination or policy.

References

Aiso S, Yamazaki K, Umeda Y, Asakura M, Kasai T, Takaya M, Toya T, et al. 2010. Pulmonary toxicity of intratracheally instilled multiwall carbon nanotubes in male Fischer 344 rats. Ind Health 48:783–795.

Asakura M, Sasaki T, Sugiyama T, Takaya M, Koda S, Nagano K, et al. 2010. Genotoxicity and cytotoxicity of multi-wall carbon nanotubes in cultured Chinese hamster lung cells in comparison with chrysotile A fibers. J Occup Health 52:155–166.

Aust A. 1994. The role of iron in asbestos induced cancer. In: Davis JMG, Jaurand M-C, editors. Cellular and Molecular Effects of Mineral and Synthetic Dusts and Fibers. NATO ASI Series. Vol. H85. Berlin: Springer-Verlag. pp 53–61.

Burrows CJ, Muller JG, Kornyushyna O, Luo W, Duarte V, Leipold MD, et al. 2002. Structure and potential mutagenicity of new hydantoin products from guanosine and 8-oxo-7,8-dihydroguanine oxidation by transition metals. Environ Health Perspect 110 (Suppl 5):713–717.

Cadet J, Berger M, Buchko GW, Joshi PC, Raoul S, Ravanat JL. 1994. 2,2-Diamino-4-[(3,5-di-O-acetyl-2-deoxy-.beta.-D-erythro- pentofuranosyl)amino]-5-(2H)-oxazolone: a novel and predominant radical oxidation product of 3',5'-di-O-acetyl-2'-deoxyguanosine. J Am Chem Soc 116:7403–7404.

Carr GJ, Gorelick NJ. 1996. Mutational spectra in transgenic animal research: data analysis and study design based upon the mutant or mutation frequency. Environ Mol Mutagen 28:405–413.

Chen CH, Su HC, Chuang SC, Yen SJ, Chen YC, Lee YT, et al. 2010. Hydrophilic modification of neural microelectrode arrays based on multi-walled carbon nanotubes. Nanotechnology 21:485501.

Deng ZJ, Liang M, Monteiro M, Toth I, Minchin RF. 2011. Nanoparticle-induced unfolding of fibrinogen promotes Mac-1 receptor activation and inflammation. Nat Nanotechnol 6:39–44.

Ellinger-Ziegelbauer H, Pauluhn J. 2009. Pulmonary toxicity of multi-walled carbon nanotubes (Baytubes) relative to alpha-quartz following a single 6h inhalation exposure of rats and a 3 months post-exposure period. Toxicology 266:16–29.

Fenoglio I, Greco G, Tomatis M, Muller J, Raymundo-Piñero E, Béguin F, et al. 2008. Structural defects play a major role in the acute lung toxicity of multiwall carbon nanotubes: physicochemical aspects. Chem Res Toxicol 21:1690–1697.

Ghosh M, Chakraborty A, Bandyopadhyay M, Mukherjee A. 2011. Multi-walled carbon nanotubes (MWCNT): induction of DNA damage in plant and mammalian cells. J Hazard Mater. 197:327–36.

Goyal RN, Jain N, Garg DK. 1997. Electrochemical and enzymic oxidation of guanosine and 8-hydroxyguanosine and the effects of oxidation products in mice. Bioelectrochemistry Bioenerg 43:105–114.

Jacobsen NR, White PA, Gingerich J, Møller P, Saber AT, Douglas GR, et al. 2011. Mutation spectrum in FE1-MUTA(TM) Mouse lung epithelial cells exposed to nanoparticulate carbon black. Environ Mol Mutagen 52:331–337.

Kino K, Ito N, Sugasawa K, Sugiyama H, Hanaoka F. 2004. Translesion synthesis by human DNA polymerase eta across oxidative products of guanine. Nucleic Acids Symp Ser 48:171–172.

Kino K, Sugiyama H. 2001. Possible cause of G-C->C-G transversion mutation by guanine oxidation product, imidazolone. Chem Biol 8:369–378.

Kino K, Sugiyama H. 2005. UVR-induced G-C to C-G transversions from oxidative DNA damage. Mutat Res 571:33–42.

Kornyushyna O, Berges AM, Muller JG, Burrows CJ. 2002. In vitro nucleotide misinsertion opposite the oxidized guanosine lesions spiroiminodihydantoin and guanidinohydantoin and DNA synthesis past the lesions using Escherichia coli DNA polymerase I (Klenow fragment). Biochemistry 41:15304–15314.

Li S, He P, Dong J, Guo Z, Dai L. 2005. DNA-directed self-assembling of carbon nanotubes. J Am Chem Soc. 127:14–5.

Ma-Hock L, Treumann S, Strauss V, Brill S, Luizi F, Mertler M, et al. 2009. Inhalation toxicity of multiwall carbon nanotubes in rats exposed for 3 months. Toxicol Sci 112:468–481.

Migliore L, Saracino D, Bonelli A, Colognato R, D'Errico MR, Magrini A, et al. 2010. Carbon nanotubes induce oxidative DNA damage in RAW 264.7 cells. Environ Mol Mutagen 51 (4):294–303.

Monteiro-Riviere NA, Inman AO, Wang YY, Nemanich RJ. 2005. Surfactant effects on carbon nanotube interactions with human keratinocytes. Nanomedicine 1:293–299.

Morimoto Y, Hirohashi M, Ogami A, Oyabu T, Myojo T, Todoroki M, et al. 2011. Pulmonary toxicity of well-dispersed multi-wall carbon nanotubes following inhalation and intratracheal instillation. Nanotoxicology; doi: 10.3109/17435390.2011.594912, 29 June 2011.

Moriya M. 1993. Single-stranded shuttle phagemid for mutagenesis studies in mammalian cells: 8-oxoguanine in DNA induces targeted G.C->T.A transversions in simian kidney cells. Proc Natl Acad Sci USA 90:1122–1126.

Mossman BT, Gee BL. 1993. Pulmonary reactions and mechanisms of toxicity of inhaled fibers. In: Gardner DE, et al. editors. Toxicology of the Lung. 2nd ed. New York: Raven Press. pp 371–387.

Muller J, Decordier I, Hoet PH, Lombaert N, Thomassen L, Huaux F, et al. 2008. Clastogenic and aneugenic effects of multi-wall carbon nanotubes in epithelial cells. Carcinogenesis 29:427–433.

Nohmi T, Masumura K. 2005. Molecular nature of intrachromosomal deletions and base substitutions induced by environmental mutagens. Environ Mol Mutagen 45:150–161.

Nohmi T, Suzuki T, Masumura K. 2000. Recent advances in the protocols of transgenic mouse mutation assays. Mutat Res 455:191–215.

Pacurari M, Castranova V, Vallyathan V. 2010. Single- and multi-wall carbon nanotubes versus asbestos: are the carbon nanotubes a new health risk to humans? J Toxicol Environ Health A 73:378–395.

Patlolla A, Hussain SM, Schlager JJ, Patlolla S, Tchounwou PB. 2010c. Comparative study of the clastogenicity of functionalized and non-functionalized multiwalled carbon nanotubes in bone marrow cells of Swiss-Webster mice. Environ Toxicol 25:608–621.

Patlolla A, Knighten B, Tchounwou P. 2010a. Multi-walled carbon nanotubes induce cytotoxicity, genotoxicity and apoptosis in normal human dermal fibroblast cells. Ethn 20(Suppl 1):S1-65–S1-72.

Patlolla A, Patlolla B, Tchounwou P. 2010b. Evaluation of cell viability, DNA damage, and cell death in normal human dermal fibroblast cells induced by functionalized multiwalled carbon nanotube. Mol Cell Biochem 338:225–232.

Pauluhn J. 2010a. Subchronic 13-week inhalation exposure of rats to multiwalled carbon nanotubes: toxic effects are determined by density of agglomerate structures, not fibrillar structures. Toxicol Sci 113:226–242.

Pauluhn J. 2010b. Multi-walled carbon nanotubes (Baytubes): approach for derivation of occupational exposure limit. Regul Toxicol Pharmacol 57:78–89.

Poland CA, Duffin R, Kinloch I, Maynard A, Wallace WA, Seaton A, et al. 2008. Carbon nanotubes introduced into the abdominal cavity of mice show asbestos-like pathogenicity in a pilot study. Nat Nanotechnol 3:423–428.

Pollack M, Oe T, Lee SH, Silva Elipe MV, Arison BH, Blair IA. 2003. Characterization of 2'-deoxycytidine adducts derived from 4-oxo-2-nonenal, a novel lipid peroxidation product. Chem Res Toxicol 16:893–900.

Pollack M, Yang IY, Kim HY, Blair IA, Moriya M. 2006. Translesion DNA Synthesis across the heptanone-etheno-2'-deoxycytidine adduct in cells. Chem Res Toxicol 19:1074–1079.

Porter DW, Hubbs AF, Mercer RR, Wu N, Wolfarth MG, Sriram K, et al. 2010. Mouse pulmonary dose- and time course-responses induced by exposure to multi-walled carbon nanotubes. Toxicology 269:136–147.

Porter DW, Millecchia LL, Robinson VA, Hubbs A, Willard P, Pack D, et al. 2002. Enhanced nitric oxide and reactive oxygen species production and damage after inhalation of silica. Am J Physiol Lung Cell Mol Physiol 283:L485–L493.

Porter DW, Millecchia LL, Willard P, Robinson VA, Ramsey D, McLaurin J, et al. 2006. Nitric oxide and reactive oxygen species production causes progressive damage in rats after cessation of silica inhalation. Toxicol Sci 90(1):188–197.

Reddy AR, Reddy YN, Krishna DR, Himabindu V. 2012. Pulmonary toxicity assessment of multiwalled carbon nanotubes in rats following intratracheal instillation. Environ Toxicol 27:211–219.

Rindgen D, Lee SH, Nakajima M, Blair IA. 2000. Formation of a substituted 1,N(6)-etheno-2'-deoxyadenosine adduct by lipid hydroperoxide-mediated generation of 4-oxo-2-nonenal. Chem Res Toxicol 13:846–852.

Rindgen D, Nakajima M, Wehrli S, Xu K, Blair IA. 1999. Covalent modifications to 2'-deoxyguanosine by 4-oxo-2-nonenal, a novel product of lipid peroxidation. Chem Res Toxicol 12:1195–1204.

Ryman-Rasmussen JP, Cesta MF, Brody AR, Shipley-Phillips JK, Everitt JI, Tewksbury EW, et al. 2009. Inhaled carbon nanotubes reach the subpleural tissue in mice. Nat Nanotechnol 4:747–751.

Sakamoto Y, Nakae D, Fukumori N, Tayama K, Maekawa A, Imai K, et al. 2009. Induction of mesothelioma by a single intrascrotal administration of multi-wall carbon nanotube in intact male Fischer 344 rats. J Toxicol Sci 34:65–76.

Sakamoto Y, Nakae D, Hagiwara Y, Satoh K, Ohashi N, Fukamachi K, et al. 2010. Serum level of expressed in renal carcinoma (ERC)/mesothelin in rats with mesothelial proliferative lesions induced by multi-wall carbon nanotube (MWCNT). J Toxicol Sci 35:265–270.

Sargent LM, Shvedova AA, Hubbs AF, Salisbury JL, Benkovic SA, Kashon ML, et al. 2009. Induction of aneuploidy by single-walled carbon nanotubes. Environ Mol Mutagen 50:708–717.

Shibutani S, Takeshita M, Grollman AP. 1991. Insertion of specific bases during DNA synthesis past the oxidation-damaged base8-oxodG. Nature 349:431–434.

Tabet L, Bussy C, Setyan A, Simon-Deckers A, Rossi MJ, Boczkowski J, et al. 2011. Coating carbon nanotubes with a polystyrene-based polymer protects against pulmonary toxicity. Part Fibre Toxicol 8:3.

Takagi A, Hirose A, Nishimura T, Fukumori N, Ogata A, Ohashi N, et al. 2008. Induction of mesothelioma in p53+/- mouse by intraperitoneal application of multi-wall carbon nanotube. J Toxicol Sci 33:105–116.

Takaya M, Serita F, Yamazaki K, Aiso S, Kubota H, Asakura M, et al. 2010. Characteristics of multiwall carbon nanotubes for an intratracheal instillation study with rats. Ind Health 48:452–459.

Totsuka Y, Higuchi T, Imai T, Nishikawa A, Nohmi T, Kato T, et al. 2009. Genotoxicity of nano/microparticles in in vitro micronuclei, in vivo comet and mutation assay systems. Part Fibre Toxicol 6:23.

Totsuka Y, Kato T, Masuda S, Ishino K, Matsumoto Y, Goto S, et al. 2010. In vitro and in vivo genotoxicity induced by fullerene (C60) and kaolin. Genes Environ 33:14–20.

Wick P, Manser P, Limbach LK, Dettlaff-Weglikowska U, Krumeich F, Roth S, et al. 2007. The degree and kind of agglomeration affect carbon nanotube cytotoxicity. Toxicol Lett 168:121–131.

Wirnitzer U, Herbold B, Voetz M, Ragot J. 2009. Studies on the in vitro genotoxicity of baytubes, agglomerates of engineered multi-walled carbon-nanotubes (MWCNT). Toxicol Lett 186:160–165.

Wörle-Knirsch JM, Pulskamp K, Krug HF. 2006. Oops they did it again! Carbon nanotubes hoax scientists in viability assays. Nano Lett 6:1261–1268.

Yang IY, Hashimoto K, de Wind N, Blair IA, Moriya M. 2009. Two distinct translesion synthesis pathways across a lipid peroxidation-derived DNA adduct in mammalian cells. J Biol Chem 284:191–198.

Ye Y, Muller JG, Luo W, Mayne CL, Shallop AJ, Jones RA, et al. 2003. Formation of 13C-, 15N-, and 18O-labeled guanidinohydantoin from guanosine oxidation with singlet oxygen. Implications for structure and mechanism. J Am Chem Soc 125:13926–13927.

Supplementary material available online

Supplementary Table I, Figure 1.

The Journal of Toxicological Sciences (J. Toxicol. Sci.)
Vol.38, No.3, 503-511, 2013

Original Article

Genotoxicity and reactive oxygen species production induced by magnetite nanoparticles in mammalian cells

Masanobu Kawanishi[1], Sayaka Ogo[1], Miho Ikemoto[1], Yukari Totsuka[2], Kousuke Ishino[2], Keiji Wakabayashi[3] and Takashi Yagi[1,4]

[1]Graduate School of Science and Radiation Research Center, Osaka Prefecture University, 1-2 Gakuen-cho, Sakai, Osaka 599-8570, Japan
[2]Division of Cancer Development System, National Cancer Center Research Institute, 5-1-1 Tsukiji, Chuo-ku, Tokyo, 104-0045, Japan
[3]Graduate School of Nutritional and Environmental Sciences, University of Shizuoka, 52-1 Yada, Suruga-ku, Shizuoka, 422-8002, Japan
[4]Department of Life Science, Dongguk University Seoul, 26, 3 Pil-dong, Jung-gu, Seoul, 100-715, Korea

(Received February 21, 2013; Accepted March 7, 2013)

ABSTRACT — We examined the genotoxicity of magnetite nanoparticles (primary particle size: 10 nm) on human A549 and Chinese hamster ovary (CHO) AA8 cells. Six hours' treatment with the particles dose-dependently increased the frequency of micronuclei (MN) in the A549 and CHO AA8 cells up to 5.2% and 5.0% at a dose of 200 μg/ml (34 μg/cm^2), respectively. In A549 cells, treatment with the nanoparticles (2 μg/ml) for 1 hr induced H2AX phosphorylation, which is suggestive of DNA double strand breaks (DSB). Treating CHO AA8 cells with 2 μg/ml (0.34 μg/cm^2) magnetite for 1 hour resulted in a five times higher frequency of sister chromatid exchange (SCE) than the control level. We detected reactive oxygen species (ROS) in CHO cells treated with the particles. These findings indicate that magnetite nanoparticles induce ROS in mammalian cells, leading to the direct or indirect induction of DSB, followed by clastogenic events including MN and SCE.

Key words: Magnetite nanoparticles, Genotoxicity, DNA damage, Reactive oxygen species, Mammalian cells

INTRODUCTION

Nanosized particles are important materials in many areas including the industrial, medical, and cosmetic fields since they have useful physical and chemical properties, such as increased chemical and/or biological reactivity, a larger active surface area, or enhanced electrical conductivity, etc. (Mazzola, 2003; Paull *et al.*, 2003; Elmore, 2003; IARC, 1996; Hoet *et al.*, 2006; Bosi *et al.*, 2003; Oberdorster *et al.*, 2005). However, these particles can be released into the environment and then inhaled by humans. Thus, occupational exposure to airborne nanoparticles has become a focus of attention in recent years. For example, their adverse effects on health have begun to be reported (Peters *et al.*, 1997; Schulz *et al.*, 2005). One of the major mechanisms by which nanosized particles cause adverse health effects is their ability to generate reactive oxygen species (ROS), which leads to oxidative stress in cells (Upadhyay *et al.*, 2003; Donaldson *et al.*, 2005). However, toxicological information on the effects of nanoparticles is still scarce (Lewinski *et al.*, 2008).

Magnetite, a mineral, is one of two common naturally occurring oxides of iron (general formula: Fe_3O_4). Nanosized magnetite particles have received special interest in the biological and medical science fields due to their superior biocompatibility, chemical stability in physiological media, and ease of production (Figuerola *et al.*, 2010). Cytotoxicity of the particles in different cell lines has been reported but to a varying extent (Ankamwar *et al.*, 2010; Hussain *et al.*, 2005; Pickard and Chari, 2010). Instillation of the particles in mice increased expression of pro-inflammatory cytokines and reduced intracellular glutathione (Park *et al.*, 2010). Several studies have examined the genotoxicity of nanosized magnetite particles; however, the data about this subject are incomplete and do

Correspondence: Takashi Yagi (E-mail: yagi-t@riast.osakafu-u.ac.jp)

not give a coherent picture. Konczol *et al.* (2011) reported that treatment with magnetite nanoparticles induced ROS production, DNA damage as measured with the comet assay, and micronuclei (MN) formation in human alveolar epithelial-like type-II cells (A549 cells). On the other hand, they did not cause a significant increase in DNA damage or MN formation in Syrian hamster embryo cells (Guichard *et al.*, 2012). Size of the particles used by both groups was almost the same; Konczol *et al.* used the particles with 20-60 nm and Guichard *et al.* used those with 27 ± 8 nm. Their chemical purities were similar as well (≥ 98% and > 99.5% in experiments by Konczol *et al.* and Guichard *et al.*, respectively). Furthermore, both groups reported that the nanoparticles were mainly present as aggregates or agglomerates in cell culture media, and they were incorporated into the cells (Konczol *et al.*, 2011; Guichard *et al.*, 2012). Thus, further toxicity studies are required to increase our understanding of the toxic potential of magnetite nanoparticles.

The present study aims to examine the genotoxicity/clastogenicity of nanosized magnetite particles in cultured human and rodent cells using the *in vitro* MN test and sister chromatid exchange (SCE) test. We also assessed the phosphorylation of H2AX (γH2AX), a marker of DNA double strand breaks (DSB), and ROS production in cells treated with the particles.

MATERIALS AND METHODS

Nanomaterial

Magnetite nanoparticles with a primary particle size of 10 nm were purchased from Toda Kogyo Corp. (Hiroshima, Japan). Their specific surface area was 116 m^2/g (disclosed by Toda Kogyo). The particles were suspended in water at a concentration of 2 mg/ml. For the cell treatments, the suspension was further diluted with saline (Otsuka Pharmaceutical Co. Ltd., Tokyo, Japan) containing 0.05% of Tween 80 (Nacalai Tesque, Kyoto, Japan) and then sonicated for 15-20 min.

Micronucleus test

The MN test was carried out as described previously (Totsuka *et al.*, 2009). Briefly, human lung carcinoma A549 cells and Chinese hamster ovary (CHO) AA8 cells obtained from the RIKEN Cell Bank (Wako, Japan) were cultured in Eagle's minimum essential medium (Nissui Pharmaceutical Co. Ltd., Tokyo, Japan) supplemented with 10% fetal bovine serum (JRH Biosciences, Lenexa, KS, USA) at 37°C in a 5% CO_2 atmosphere. The cells (A549, 7×10^5 cells/dish; CHO AA8, 4×10^5 cells/dish) were then seeded in plastic cell culture dishes (φ60 mm) one day before the treatment procedure. Suspensions of the nanoparticles were sonicated for 5-10 min at room temperature, and one volume of the suspension was mixed with 9 volumes of the culture medium supplemented with 10% fetal bovine serum (total: 3.3 ml/dish). Then, the cells were treated with the nanoparticles at the indicated concentrations for 6 hr. After being treated, the A549 and CHO AA8 cells were cultured for a further 42 or 20 hr, respectively. In the treatments involving anti-oxidants, the cells were cultured with medium containing the indicated concentration of *N*-acetylcysteine (NAC; Nacalai Tesque) or α-tocopherol (Nacalai Tesque) for 1 hr before the magnetite nanoparticle treatment. The cells were then treated with the nanoparticles for 6 hr, before being cultured for 42 hr (A549 cells) or 20 hr (CHO AA8 cells) in the presence of the anti-oxidants. Then, the cells were trypsinized, counted, and centrifuged. Growth inhibition was calculated using following the formula:

Growth rate = (the number of treated cells) ÷ (the number of non-treated cells)

The cells were then resuspended in 0.075 M KCl and incubated for 5 min, before being fixed 4 times in methanol:glacial acetic acid (3:1) and washed with methanol containing 1% acetic acid. Finally, the cells were resuspended in methanol containing 1% acetic acid. The cell solution was dropped onto slides, and then the nuclei were stained by mounting the cells with 40 μg/ml acridine orange (Nacalai Tesque) solution and immediately observed by fluorescence microscopy using blue excitation. The number of cells with MN was recorded based on the observation of 1,000 interphase cells.

Detection of γH2AX

To detect DSB, immunostaining of γH2AX was carried out as described previously (Shimohara *et al.*, 2008). Briefly, the A549 cells were seeded on glass slides at a density of 4×10^5 cells/ml. The cells were then exposed to the nanoparticles for 1 hr as described above, but with serum-free medium, before being cultured for 1 hr with medium containing 10% fetal bovine serum. Etoposide (final concentration: 100 μg/ml; Sigma-Aldrich Japan, Tokyo, Japan) was used as a positive control. The cells were fixed on the glass slides with methanol, rinsed with ice-cold PBS (Takara Bio Inc., Shiga, Japan), and immersed in PBS containing 5% Triton X100 (ICN Biomedicals Inc., Irvine, CA, USA) for 30 min. The cells were then rinsed with ice-cold PBS and kept in PBS containing 5% bovine serum albumin (Sigma-Aldrich Japan) for 18 hr at room temperature, before being rinsed in PBS and treated with an anti-phospho-H2AX mouse

monoclonal antibody (2 μg/ml in PBS; 05-636; Upstate Biotechnology Inc., Lake Placid, NY, USA) for 1 hr at room temperature. Next, the cells were rinsed with ice-cold PBS and treated with the secondary antibody, Alexa Flour 488 anti-mouse IgG (1/1,000 diluted in PBS; A11029; Molecular Probe, Junction City, OR, USA), for 1 hr. After the cells had been rinsed with ice-cold PBS, they were soaked in Vectashield mounting solution containing 4',6-diamino-2-phenylindole dihydrochloride (DAPI) (H-1200; Vector Laboratories, Inc., Burlingame, CA, USA) and overlaid with a cover glass. Fluorescent images of the cell nuclei were obtained at a magnification of × 1,000 using a fluorescence microscope (BX-URA2; Olympus Co., Tokyo, Japan) and a cooled CCD camera (VB-7000; Keyence Co., Osaka, Japan). The DAPI-stained nuclei and γH2AX foci appeared blue and green, respectively. Thus, the blue and green areas of each nucleus were measured using an image analyzing system (VH-H1A5; Keyence Co.). The value of the green area divided by the total (blue+green) area was used to represent the relative level of H2AX phosphorylation.

SCE test

The SCE test was performed as described previously (Kato *et al.*, 2012). Briefly, CHO AA8 cells were cultured in RPMI 1640 (Sigma-Aldrich Japan) supplemented with 10% fetal bovine serum (JRH Biosciences) at 37°C in a 5% CO_2 atmosphere. The cells were treated with the nanoparticles for 1 hr as described above and then cultured in medium containing 10% serum and 10 μg/ml 5-bromodeoxyuridine (Sigma-Aldrich Japan) for 26 hr. Colcemid (Nacalai Tesque) was added for the last 2 hr at a final concentration of 60 ng/ml. The cells were then trypsinized and centrifuged, resuspended in 0.075 M KCl, and incubated for 30 min, before being fixed four times in methanol:glacial acetic acid (3:1). The cell solution was dropped onto slides in a HANABI Metaphase Spreader (AD Science Technology, Funabashi, Japan). The slides were then soaked in 50 μg/ml Hoechst #33258 (Sigma-Aldrich, St. Louis, MO, USA), before being covered with 0.01 M sodium phosphate buffer (pH 7.6) and cover glasses and irradiated with black light at 365 nm for 3 hr. Subsequently, the slides were stained with 6% Giemsa stain (Merck KGaA, Darmstadt, Germany) in 0.06 M sodium phosphate buffer (pH 6.4) for 15 min. SCE was scored under a microscope. At least 50 cells were observed in each experiment.

Detection of ROS

CellROX Deep Red Reagent (Life Technologies, Carlsbad, CA, USA) was used to detect ROS according to the manufacturer's instructions. Briefly, CHO AA8 cells (2×10^5 cells/well) were seeded in 6-well plates a day before the experiment. The cells were treated with the nanoparticles for 1 hr, as described in the section "Detection of γH2AX", and then CellROX Deep Red Reagent was added to them at a final concentration of 5 μM, before the cells were incubated with the nanoparticles for further 30 min at 37°C. Then, the cells were washed with PBS and recovered with trypsin treatment. In the experiments involving anti-oxidant exposure (NAC, α-tocopherol, or ascorbic acid; Nacalai Tesque), the cells were cultured with medium containing the indicated concentrations of anti-oxidants for 1 hr before the treatment. Then, the cells were treated with the nanoparticles for 1 hr and cultured further with the nanoparticles and CellROX Deep Red Reagent for 0.5 hr in the presence of the anti-oxidant. The fluorescence intensity produced by the CellROX Deep Red Reagent was determined with flow cytometry (FCM) (Accuri C6 flow cytometer; Becton Dickinson, Franklin Lakes, NJ, USA). At least 10,000 cells per sample were analyzed.

Statistical analysis

The Tukey-Kramer method or Student's t-test was used to compare the difference in means between the treated and control groups using R 2.10.1 or Microsoft Excel 2004 software, respectively. One-way analysis of variance (ANOVA) was carried out using Microsoft Excel 2004 software in order to show the effect of concentration, where appropriate. A p value < 0.05 was considered statistically significant.

RESULTS AND DISCUSSION

Induction of micronucleus formation

The MN-inducing activity of the magnetite nanoparticles was examined using the human lung cancer cell line A549. Six hours' treatment with 200 μg/ml (34 μg/cm²) magnetite inhibited the growth of the A549 cells by 69.2% (data not shown). As shown in Fig. 1, the magnetite nanoparticles increased the number of micronucleated cells in a dose-dependent manner. The background frequency of micronucleated cells was 1.8%, and the frequency rose to 5.2% at a magnetite concentration of 200 μg/ml (34 μg/cm²). The increase in the frequency of micronucleated cells was statistically significant ($p < 0.05$) at all of the magnetite particle concentrations tested. This confirmed that magnetite nanoparticles induce MN formation in A549 cells, as was reported by Konczol *et al.* (2011). Note that they did not observe MN induction after low dose exposure (1 μg/cm²